ENVIRONMENTAL RESEARCH
LETTERS

LETTER • OPEN ACCESS

Using strontium isotopes to trace dust from a drying Great Salt Lake to adjacent urban areas and mountain snowpack

Environmental Research Letters

LETTER

Using strontium isotopes to trace dust from a drying Great Salt Lake to adjacent urban areas and mountain snowpack

Gregory T Carling[1], Diego P Fernandez[2], Kevin A Rey[1], Colin A Hale[1], Michael M Goodman[1] and Stephen T Nelson[1]

[1] Department of Geological Sciences, Brigham Young University, Provo, UT, United States of America
[2] Department of Geology & Geophysics, University of Utah, Salt Lake City, UT, United States of America

E-mail: greg.carling@byu.edu

OPEN ACCESS

RECEIVED
9 July 2020

REVISED
29 September 2020

ACCEPTED FOR PUBLICATION
9 October 2020

PUBLISHED
23 November 2020

Keywords: Mineral dust, playas, $^{87}Sr/^{86}Sr$, carbonate minerals, snowpack, urban dust, Great Salt Lake

Supplementary material for this article is available online

Abstract

With the desiccation of saline lakes around the globe, it is increasingly important to quantify the impacts of playa dust on downwind urban areas and mountain snowpack. In this study, we used $^{87}Sr/^{86}Sr$ ratios of carbonate minerals to trace dust from playas to urban areas and mountain snowpack. We focused on dust contributions from Great Salt Lake (GSL), in northern Utah, USA, which recently reached historic lows in water levels exposing large areas of dry lakebed. We measured $^{87}Sr/^{86}Sr$ ratios in dust from GSL, Sevier Dry Lake (SDL), and other playas across western Utah and compared them to $^{87}Sr/^{86}Sr$ ratios in dust across the urban Wasatch Front and mountain snowpack collected seasonally from 2015–2018. Dust from GSL had unique $^{87}Sr/^{86}Sr$ ratios (~0.715) relative to SDL (~0.710) and other playas (~0.711 to 0.712), providing a potentially powerful tool for tracing GSL dust to downwind areas. Dust deposition had $^{87}Sr/^{86}Sr$ ratios ranging from ~0.710 to ~0.712 in the urban area and snowpack, within the range of playa dust sources. Using a simple two-endmember mixing model considering only GSL and SDL as sources, GSL contributed 5% of the dust flux to the southern Wasatch Front (Provo) and between 30%–34% of the dust flux to the northern Wasatch Front (Salt Lake City, Ogden, and Logan). For mountain snowpack, GSL contributed 11% of the dust flux to the Uinta Mountains and 22% of the dust flux to the Wasatch Mountains. Dust transport modeling could be combined with $^{87}Sr/^{86}Sr$ fingerprints for source apportionment in northern Utah and other areas that are impacted by regional playa dust.

1. Introduction

Mineral dust is globally important as it affects climate and biogeochemical cycles (Engelbrecht and Derbyshire 2010, Mahowald *et al* 2010) and decreases total mountain runoff by causing earlier snowmelt that exposes plants and soils to increased evapotranspiration (Painter *et al* 2010), yet it is often difficult to identify specific dust sources. Dust storms typically contain a mixture of particles from different sources (Lawrence and Neff 2009), which may include playas, alluvial fans, sand dunes, and anthropogenically disturbed soils (Reheis and Kihl 1995, Belnap and Gillette 1997, Neff *et al* 2008, Bullard *et al* 2011). In particular, playas represent an increasing source of dust with the global desiccation of saline lakes by water diversions (Wurtsbaugh *et al* 2017). Dust is tracked using atmospheric transport modeling (Mallia *et al* 2017), satellite imagery (Hahnenberger and Nicoll 2012), geochemistry (Reheis *et al* 2002), mineralogy and particle size distributions (Munroe 2014), and isotope fingerprinting (Munroe *et al* 2019). Each of these has significant uncertainties, such that improved methods are needed for tracing dust from source-to-sink to inform strategies for mitigating dust emissions.

Strontium isotope ($^{87}Sr/^{86}Sr$) ratios are widely used for fingerprinting dust sources but have not been used to track dust from playas at a regional scale. Commonly $^{87}Sr/^{86}Sr$ ratios are analyzed on the aluminosilicate mineral fraction after removing

the carbonate minerals by rinsing with acetic acid (Biscaye *et al* 1997, Chen *et al* 2007, Palchan *et al* 2013, Zhao *et al* 2015, Gross *et al* 2016) or by checking that carbonate minerals do not exist in the samples (Zdanowicz *et al* 2006). Grain size typically affects the $^{87}Sr/^{86}Sr$ ratio of the silicate mineral fraction given high Rb concentrations and high $^{87}Sr/^{86}Sr$ ratios in clays (Chen *et al* 2007). The carbonate mineral fraction may contain important fingerprinting information in carbonate-rich dust, particularly in regions dominated by playa dust sources. For example, pedogenesis studies use $^{87}Sr/^{86}Sr$ ratios of the carbonate mineral fraction (from acetic acid leaching) and the silicate mineral fraction (from total digestion) to determine calcium sources from atmospheric inputs versus silicate weathering (Capo *et al* 1998, Capo and Chadwick 1999, Naiman *et al* 2000). Carbonate-rich playas may have unique $^{87}Sr/^{86}Sr$ ratios if the watersheds contain different bedrock types, which would make it possible to trace the carbonate fraction of dust from playa sources.

Dust storms occur frequently along the Wasatch Front in northern Utah, USA, with negative impacts on air quality and mountain snowpack (Hahnenberger and Nicoll 2012, Steenburgh *et al* 2012, Carling *et al* 2012, Reynolds *et al* 2014). Dust sources are dominated by regional playas, including Sevier Dry Lake (SDL) and the lakebed of Great Salt Lake (GSL) (Hahnenberger and Nicoll 2014, Hahnenberger and Perry 2015, Skiles *et al* 2018), which are remnants of Pleistocene Lake Bonneville (Oviatt and Shroder 2016) (figure 1). The largest dust events typically occur with strong south-southwesterly flows ahead of cold fronts, carrying dust from southwest Utah to the Wasatch Front (Steenburgh *et al* 2012, Nicoll *et al* 2020). The importance of regional playa dust inputs to the Wasatch Front, and minimal inputs from long-range global dust, is supported by grain-size distribution, mineralogy, and chemistry data (Goodman *et al* 2019) and satellite imagery (Hahnenberger and Nicoll 2014, Nicoll *et al* 2020). Due to irrigation diversions, SDL has remained dry since 1880 except during years of high snowmelt runoff (Oviatt 1988). The GSL, located immediately adjacent to two million people in the Wasatch Front, reached its lowest lake level in recorded history in November 2016 with a 50% reduction in lake area relative to 1847. The long-term decline in GSL water levels is due to water development and river diversions (Wurtsbaugh *et al* 2017). A proposed diversion on the Bear River, the largest tributary of GSL, would cause further decline in the lake level and expose another 80 km^2 of lakebed (Wurtsbaugh *et al* 2017). As water levels continue to drop, dust events may increase in frequency and intensity in the future (Skiles *et al* 2018). Ultimately, decreasing water levels on GSL could create a 'dust bowl' similar to Owens Dry Lake in California (Gill 1996, Reheis 1997, Reheis *et al* 2002, 2009).

The purpose of our study is to use $^{87}Sr/^{86}Sr$ ratios in carbonate minerals as a tracer of dust from playa sources to urban areas and mountain snowpack. Specific objectives are to: (1) evaluate the regional variability of $^{87}Sr/^{86}Sr$ ratios in carbonate minerals from playas; (2) evaluate the seasonal $^{87}Sr/^{86}Sr$ ratios of dust in urban areas and mountain snowpack downwind of the playas; and (3) quantify the amount of dust from specific playa sources using isotopic fingerprints. The study was carried out in Utah, USA, where the dust system is characterized by regional dust emissions from playas and deposition along the populated Wasatch Front (>2 million people) and the Wasatch and Uinta Mountains (Dastrup *et al* 2018, Skiles *et al* 2018, Goodman *et al* 2019) (figure 1). We hypothesized that variable $^{87}Sr/^{86}Sr$ ratios in lacustrine carbonates and modern river inflows to lakes and playas across the Bonneville Basin (Hart *et al* 2004) could be used as a tracer of dust from specific playas. Identifying the origin of dust storms is important for determining how future water diversion schemes could alter dust source regions and affect downwind populations and mountain snowpack. For example, $^{87}Sr/^{86}Sr$ ratios could help determine whether dust fluxes from GSL increase with the proposed Bear River diversion.

2. Methods

2.1. Study background

In a previous study, we investigated the geochemistry, mineralogy, and grain size of dust from the GSL lakebed and other regional dust sources, including SDL, Sevier Desert, Tule Valley, Fish Springs playa, and Wah Wah Valley (Goodman *et al* 2019). The study showed that playas are the dominant source of dust to the urban Wasatch Front and mountain snowpack, contributing up to 90% of the total dust flux. Bulk geochemistry and mineralogy were similar amongst the various dust sources, providing no diagnostic fingerprints for source apportionment. Concentrations of specific elements (e.g. V, Cd, Sb, and Se) were higher in the Wasatch Front relative to dust sources, reflecting anthropogenic inputs of these elements. Here, we expand on the dataset to explore the use of isotopic fingerprints to identify the specific playas that contribute dust to the Wasatch front, with an emphasis on quantifying dust from SDL and GSL.

2.2. Sample locations and timing

To compare the isotopic composition of dust emissions from western Utah playas with dust deposition across northern Utah, we sampled 15 representative playa dust source locations during 2016–2017, four urban sites along the Wasatch Front during 2015–2018, and dust in snowpack from the Wasatch and Uinta Mountains during springtime from 2016–2018 (figure 1). Details about sampling methods

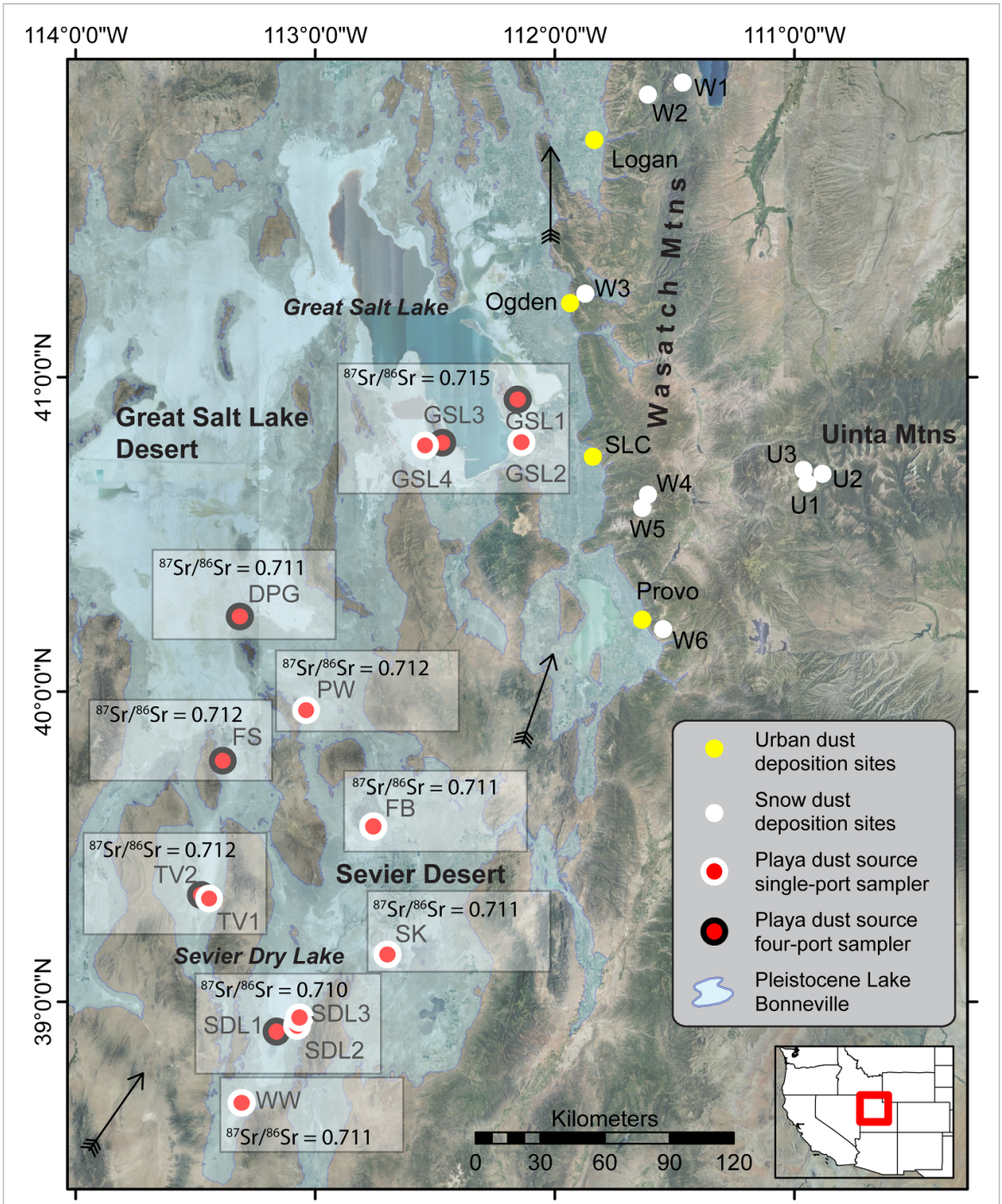

Figure 1. Playa, urban, and snow dust sampling locations in Utah, USA. Playa dust samplers were placed in dry lakebeds that are remnants of Pleistocene Lake Bonneville, including Great Salt Lake and Sevier Dry Lake. The $^{87}Sr/^{86}Sr$ values are averages for each playa, rounded to three decimal places. Urban dust collectors were placed on rooftops of buildings and snow samples were collected from mountain snowpack. Arrows indicate the south-southwesterly prevailing wind for the region (.Jewell and Nicoll 2011). Abbreviations: GSL = Great Salt Lake, DPG = Dugway Proving Ground, PW = Pismire Wash, FS = Fish Springs, TV = Tule Valley, SDL = Sevier Dry Lake, WW = Wah Wah, SK = Sunstone Knoll, FB = Fumarole Butte, W = Wasatch, U = Uintas, SLC = Salt Lake City. Figure modified after Goodman *et al* (2019).

are provided in Goodman *et al* (2019). Briefly, dust was collected from playas using passive BSNE (Big Springs Number Eight) samplers with one port at 50 cm above the ground surface (single-port sampler) or four ports at 10, 15, 20, and 50 cm (four-port sampler). Playa dust samples were collected at SDL (SDL1, SDL2, and SDL3), Tule Valley (TV1 and TV2), Wah Wah Valley (WW), Sunstone Knoll (SK), Fumarole Butte (FB), Pismire Wash (PW), Fish Springs (FS), Dugway Proving Grounds (DPG), and GSL (GSL1, GSL2, GSL3, and GSL4). The samplers were deployed for several months to collect sufficient dust for geochemical analyses, with one to three deployments per site, for a total of 69 unique samples. At the urban sites, wet and dry deposition (including dust and other aerosols) was collected at Provo, Salt Lake City (SLC), Ogden, and Logan on the roofs of four-story university buildings using a large plastic tote

covered by a screen with marbles. The samplers were placed for 2-month periods during fall 2015, spring 2016, and from June 2017 through September 2018, for a total of 35 urban samples over nine sample periods capturing seasonal and interannual variability. This included two samples that were collected for short 1-week periods at Provo when dust events were predicted in the weather forecast to compare isotopic ratios in short- and long-term samples. For snowpack, we sampled discrete dust layers at peak snowpack from the Wasatch and Uinta Mountains during spring 2016, 2017, and 2018, for a total of 22 samples, each likely representing an individual dust event including mineral particles and other aerosols.

2.3. Sample treatment and geochemical and isotopic analyses

To prepare samples for geochemical and isotopic analyses, dust was dried in a laminar flow hood at 50 °C and treated with 30% hydrogen peroxide to remove organic matter. A subset of playa dust samples was wet sieved through a 52 μm nylon mesh screen to compare the chemical and isotopic composition of 'bulk' versus 'fine' samples. Of the 69 playa samples, we analyzed 28 on the bulk fraction, 32 on the fine fraction, and 9 on both bulk and fine fractions.

Dust samples were analyzed for trace and major element concentrations and $^{87}Sr/^{86}Sr$ ratios following a four-step sequential leaching procedure. Each ~200 mg sample aliquot was reacted with 1 M ammonium acetate (buffered to pH = 7), 1 M acetic acid, 1 M nitric acid, and aqua regia (1:3 ratio of concentrated nitric acid to hydrochloric acid). The goal of the sequential leaching procedure was to target the exchangeable and water-soluble fractions with ammonium acetate, the carbonate mineral fraction with acetic acid, the feldspar and clay mineral fractions with nitric acid, and refractory minerals with aqua regia, although not all silicate minerals were completely dissolved (Lawrence *et al* 2010, Dastrup *et al* 2018, Goodman *et al* 2019). In particular, acetic acid effectively reacts with the carbonate mineral fraction of dust and soils for $^{87}Sr/^{86}Sr$ analyses (Naiman *et al* 2000). The four leachates from each sample were analyzed for trace and major element concentrations using an Agilent 7500ce quadrupole inductively coupled plasma mass spectrometer (ICP-MS), as described in Goodman *et al* (2019).

All dust samples ($n = 135$), with the exception of one snow dust sample with insufficient sample mass, were analyzed for $^{87}Sr/^{86}Sr$ ratios on the acetic acid leachate using a Thermo Scientific Neptune multi-collector ICP-MS. Additionally, to compare $^{87}Sr/^{86}Sr$ ratios within different mineral fractions, a subset of playa, urban, and snow dust samples were analyzed for $^{87}Sr/^{86}Sr$ ratios on the ammonium acetate leachate ($n = 52$) and nitric acid leachate ($n = 22$). The samples were purified inline using a Sr-FAST ion chromatographic column packed with a crown ether resin (Mackey and Fernandez 2011). During the analyses reported herein, we determined the $^{87}Sr/^{86}Sr$ ratio of the standard reference material SRM987 (certified value of 0.71034 ± 0.00026) to be 0.710293 ± 0.000013 ($n = 133$; mean ± standard deviation). Analytical precision (standard error) of all samples ranged from ±0.000003–0.000030. The $^{87}Sr/^{86}Sr$ ratios were corrected for mass bias using an exponential law, normalizing to $^{86}Sr/^{88}Sr = 0.1194$ (Steiger and Jäger 1977). Isobaric interferences on the $^{87}Sr/^{86}Sr$ ratios, such as from ^{87}Rb and ^{86}Kr, were corrected by simultaneously monitoring ^{85}Rb and ^{83}Kr using the corresponding invariant ratios of $^{87}Rb/^{85}Rb = 0.385706$ and $^{86}Kr/^{83}Kr = 1.502522$ (Steiger and Jäger 1977).

3. Results

3.1. $^{87}Sr/^{86}Sr$ ratios in dust from the playas, urban area, and mountain snowpack

Strontium isotope ($^{87}Sr/^{86}Sr$) ratios in the acetic acid leachate (or carbonate mineral fraction) ranged widely in the playa dust sources, with generally increasing $^{87}Sr/^{86}Sr$ ratios from south at SDL (~0.710) to north at GSL (~0.715) and intermediate values (~0.711 to ~0.712) in between (figure 1). Specifically, the values ranged from 0.71008 ± 0.00009 (mean ± standard error) at SDL ($n = 14$) to 0.71476 ± 0.00006 at GSL ($n = 32$), with intermediate values of 0.71178 ± 0.00010 at the other playas ($n = 32$) (figure 2). These values are averages from fine and bulk samples within each group, where fine samples were sieved to <52 μm and the bulk samples contained particles >200 μm that are likely not available for aeolian transport (Goodman *et al* 2019). To evaluate a potential grain-size effect on $^{87}Sr/^{86}Sr$ ratios, we analyzed for both fine and bulk fractions in a subset of samples ($n = 9$) with similar values in both fractions (figure 3). Further, the ammonium acetate, acetic acid, and nitric acid leachates had similar $^{87}Sr/^{86}Sr$ ratios (figure 4). In the dust samples, >83% of Sr was contained in the ammonium acetate and acetic acid leachate fractions, with up to 14% of Sr in the nitric acid and up to 3% in the aqua regia fractions (Goodman *et al* 2019).

The $^{87}Sr/^{86}Sr$ ratios in dust deposition across the Wasatch Front urban area (Provo, SLC, Ogden, and Logan) and snowpack (Wasatch and Uinta Mountains) were within the range of playa values (figure 2). At the urban sites, the $^{87}Sr/^{86}Sr$ ratios ranged from 0.71022 ± 0.00010 at Provo ($n = 10$) to 0.71169 ± 0.00013 at Ogden ($n = 8$), with SLC and Logan showing similar values as Ogden. Ratios for dust in snow were lower at the Uinta Mountains relative to the Wasatch Mountains but both were within the range of urban dust, averaging 0.71055 ± 0.00013 in the Uintas ($n = 10$) and

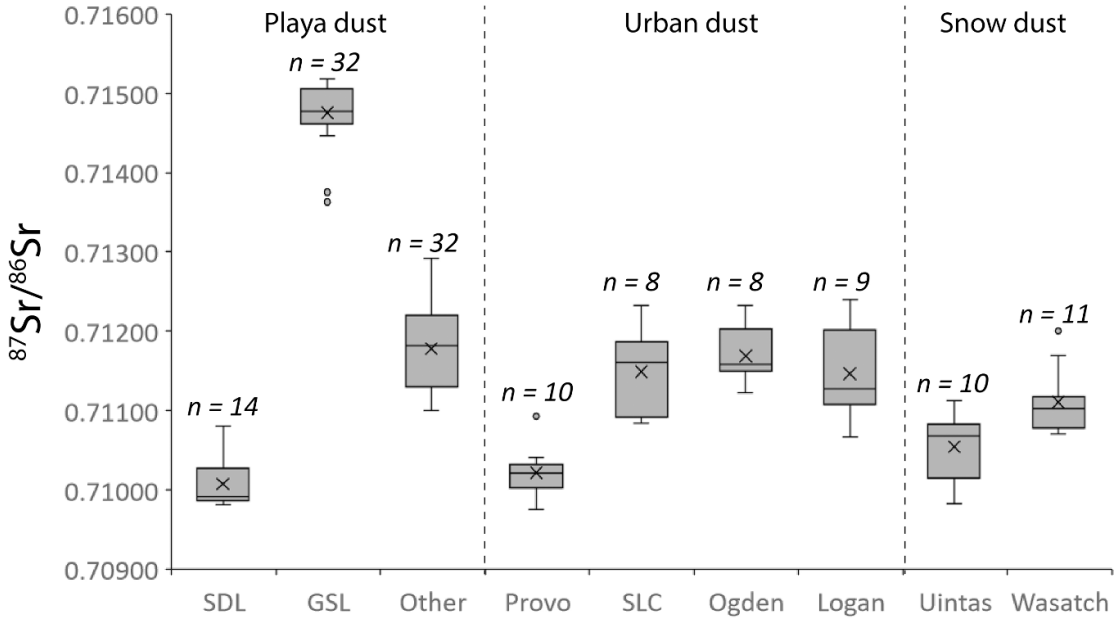

Figure 2. Box plots of $^{87}Sr/^{86}Sr$ ratios in the acetic acid leachate of dust samples from playas (Sevier Dry Lake, Great Salt Lake, other playas), the Wasatch Front urban area (Provo, Salt Lake City, Ogden, and Logan), mountain snowpack (Uintas and Wasatch). The mean values are indicated with an X and outliers are shown as dots.

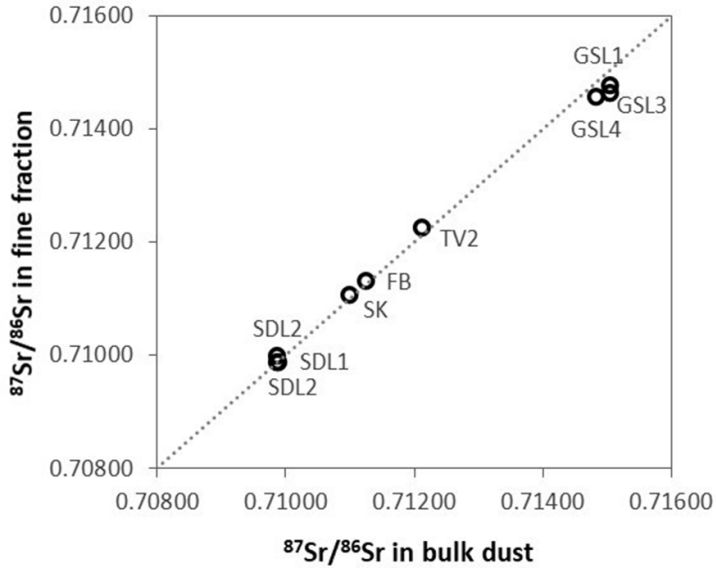

Figure 3. Sr isotope ($^{87}Sr/^{86}Sr$) ratios in the acetic acid leachate on playa dust samples in the bulk and <52 μm size fraction. Sample labels correspond to playa locations shown in figure 1. The dashed line is a 1:1 line.

0.71111 ± 0.00012 in the Wasatch (n = 11) over three sampling seasons. Raw $^{87}Sr/^{86}Sr$ ratios and geochemical data for all samples are provided in the Supplementary material (table S1 (available online at https://stacks.iop.org/ERL/15/114034/mmedia)).

3.2. Seasonal variability in $^{87}Sr/^{86}Sr$ ratios of urban dust

The $^{87}Sr/^{86}Sr$ ratio in dust varied over time at the urban sites (figure 5). Provo dust consistently had the lowest $^{87}Sr/^{86}Sr$ ratio during each sampling period. The ratios from the four urban sites converged during Feb–May 2016 and Jan–Mar 2018 but Provo still had the lowest values. During most sampling periods, there was a large separation between Provo and the other sites. The site with the highest ratio changed during each sampling period, with SLC, Ogden, and Logan showing the highest values but the most variability in $^{87}Sr/^{86}Sr$ ratios. Provo, the southernmost sampling site in the urban area, had $^{87}Sr/^{86}Sr$ ratios similar to SDL while the $^{87}Sr/^{86}Sr$ ratios at SLC, Ogden, and Logan were more similar to GSL and other playas. The 1-week sample from Provo had the same $^{87}Sr/^{86}Sr$ ratio as the corresponding seasonal

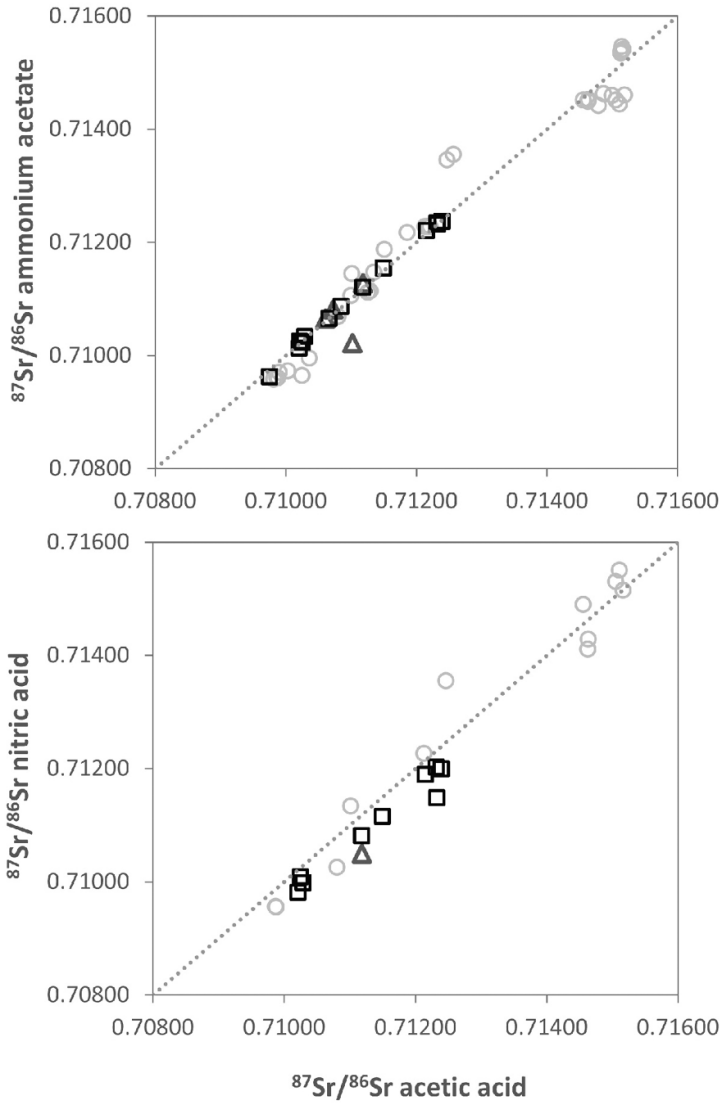

Figure 4. Sr isotope ($^{87}Sr/^{86}Sr$) ratios in playa (circles), urban (squares), and snow (triangles) dust samples ammonium acetate versus acetic acid leachates (top) and nitric acid versus acetic acid leachates (bottom). The dashed line is a 1:1 line.

sample during Sep–Nov 2015 but was relative lower during Feb–May 2016.

4. Discussion

4.1. Variability in the $^{87}Sr/^{86}Sr$ ratio of playa dust sources

Strontium isotope ($^{87}Sr/^{86}Sr$) ratios varied from 0.710 in the Sevier Desert to 0.715 at GSL in the carbonate mineral fraction (figures 1 and 2), which is a wide range in values (relative to analytical errors on the order of ±0.00001) that provides leverage for discriminating the relative importance of dust from each source (Chen *et al* 2007). Other playas from the GSL Desert and Sevier Desert contained intermediate $^{87}Sr/^{86}Sr$ ratios of ~0.711 or ~0.712 (figure 1). The variability in $^{87}Sr/^{86}Sr$ ratios (increasing values from south to north) is primarily a result of lacustrine carbonate mineral precipitation from Lake Bonneville and subsequent lakes over time depending on river inflows and separation of the lake into different basins (Hart *et al* 2004). The Bear River, which is the dominant Sr source to GSL, contains elevated $^{87}Sr/^{86}Sr$ ratios relative to the Sevier River, the dominant Sr source to SDL. The high $^{87}Sr/^{86}Sr$ ratio in the Bear River is due to thermal spring and groundwater additions to the lower section of the river, including Crystal Hot Springs with a Sr concentration of 36 ppm and $^{87}Sr/^{86}Sr$ ratio of 0.72341 (Hart *et al* 2004). Two unusually low values at GSL (figure 2) are from GSL2, which may reflect the mixing of dust inputs from the Kennecott tailings pile or other localized sources on the south end of the lake. However, even the two 'low' values at GSL are higher than $^{87}Sr/^{86}Sr$ ratios from any other sources.

4.2. Using $^{87}Sr/^{86}Sr$ ratios to quantify dust inputs from the dry lakebed of Great Salt Lake

With the newly developed $^{87}Sr/^{86}Sr$ isotopic fingerprinting tool, we can begin to identify specific dust

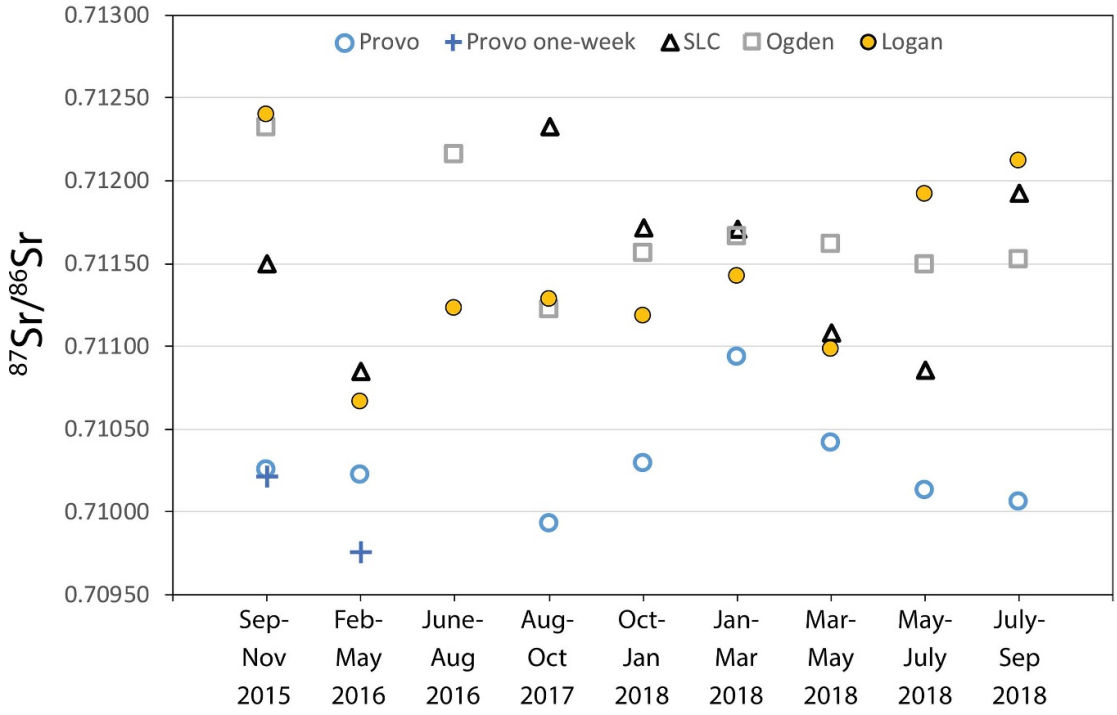

Figure 5. Time series of $^{87}Sr/^{86}Sr$ ratios in the acetic acid leachate fraction of urban dust samples collected from Provo, Salt Lake City, Ogden, and Logan.

sources that affect the Wasatch Front and monitor changes over time. In a previous study, we showed that regional playas are responsible for most of the dust mass deposited along the Wasatch Front (Goodman *et al* 2019). Other studies highlight the importance of regional playas contributing to Wasatch Front dust (Hahnenberger and Nicoll 2014, Nicoll *et al* 2020). Thus, tracking playa sources using $^{87}Sr/^{86}Sr$ ratios would describe a majority of regional dust transport and deposition. The similarity in $^{87}Sr/^{86}Sr$ ratios regardless of grain-size fraction (figure 3) or leaching fraction (figure 4) further strengthens the use of an $^{87}Sr/^{86}Sr$ fingerprint for playa dust sources. The similarities in $^{87}Sr/^{86}Sr$ ratios among size fractions and the readily leached mineral fractions may be a result of mineral precipitation in the playa environment, with mineral precipitation resulting in the same $^{87}Sr/^{86}Sr$ ratio regardless of mineral grain size (e.g. precipitation of fine carbonate mud and large ooids) or mineral phase. Further, the nitric acid leachate fraction may contain trace amounts of unreacted carbonate minerals, such as dolomite, that dominate the $^{87}Sr/^{86}Sr$ ratio over the feldspar or clay fraction.

The observed $^{87}Sr/^{86}Sr$ ratios in the Wasatch Front urban area and mountain snowpack could be explained as a mixture of inputs from SDL, GSL, and/or other playas. As a first attempt at source apportionment, we used a two-endmember mixing model to compare the relative amount of dust from SDL and GSL, assuming these are the two major sources of dust to the Wasatch Front (Hahnenberger and Nicoll 2014, Hahnenberger and Perry 2015, Skiles *et al* 2018, Nicoll *et al* 2020). Other playas besides SDL and GSL contribute dust to the Wasatch Front, yet the $^{87}Sr/^{86}Sr$ ratios for Provo dust were nearly identical to the $^{87}Sr/^{86}Sr$ ratios for SDL, highlighting the importance of SDL as the primary dust source. Sites further north (SLC, Ogden, and Logan) had higher $^{87}Sr/^{86}Sr$ ratios that could reflect additional inputs from GSL or other playas (figure 2). Given their proximity to GSL, it seems likely that at least a portion of the dust is from the GSL lakebed, contributing to the higher $^{87}Sr/^{86}Sr$ ratios at SLC, Ogden, and Logan relative to Provo. The two-endmember mixing model results should be considered maximum values for GSL dust inputs since other playa sources also contributed to the observed $^{87}Sr/^{86}Sr$ ratios, but are at least an approximation of the potential impact of GSL dust.

To quantify seasonal contributions of GSL dust to each urban area and to mountain snowpack, the two-endmember mixing model (Naiman *et al* 2000) included average $^{87}Sr/^{86}Sr$ values from GSL and SDL:

$$\left(^{87}Sr/^{86}Sr\right)_{urban\,or\,snow\,dust} = x\left(^{87}Sr/^{86}Sr\right)_{GSL} + (1-x)\left(^{87}Sr/^{86}Sr\right)_{SDL}$$

where $(^{87}Sr/^{86}Sr)_{GSL}$ is the average value of 0.71476 for GSL, $(^{87}Sr/^{86}Sr)_{SDL}$ is the average value of 0.71008 for SDL, and x is the fraction of GSL dust contributing to observed values in urban or snow dust. A major assumption in this mixing model is that Sr concentrations are equal across the playa dust sources since

isotopic mixing is a function of both Sr concentrations and $^{87}Sr/^{86}Sr$ ratios. From the samples we collected, Sr concentrations were similar for GSL and SDL in the ammonium acetate fraction but much higher for GSL in the acetic acid fraction (supplementary material, figure S1). Thus, using Sr concentrations from the acetic acid fraction in the mixing equation would result in lower estimates of GSL dust inputs. The mineralogy and Sr concentration of playa soils and dust depends on the location within the playa that was sampled. Therefore, the relative differences in Sr concentrations is likely an artifact of under-sampling because we only had four sampling locations at GSL and three sampling locations at SDL. If we were able to sample dust emissions across the entire playa surface at GSL and SDL, we assume that both playas would have similar Sr concentrations. Clearly, additional work is needed to characterize spatial heterogeneity in Sr concentrations across dust-producing areas of the playas. On the other hand, $^{87}Sr/^{86}Sr$ ratios from our limited sampling at each playa are likely representative of the entire playa surface since these values in the readily leachable fraction represent Sr that precipitated from well-mixed water, regardless of the dominant mineralogy upwind of the sampling location.

The mixing model shows seasonal and spatial variability in the amount of GSL dust inputs to the Wasatch Front over the 3-year period (supplementary material, table S2). The fraction of GSL dust ranged from 0%–18% at Provo, 16%–48% at SLC, 24%–48% at Ogden, and 12%–49% at Logan during the study period. On average, GSL contributed 5% of the dust to Provo and between 30%–34% of the dust to SLC, Ogden, and Logan. These values show a clear trend from south to north, with Provo receiving less dust from GSL than SLC, Ogden, or Logan. This is expected because the dust storms are typically driven by south-southwesterly winds that would send GSL dust to SLC, Ogden, and Logan but not to Provo (Jewell and Nicoll 2011). At Provo, the dust is likely sourced from SDL since the Provo $^{87}Sr/^{86}Sr$ values matched so closely with SDL and were lower than GSL and other playas. For snowpack, GSL dust contributed 0%–22% (average: 11%) of the dust to the Uinta Mountains and 13%–41% (average: 22%) of the dust to the Wasatch Mountains. These differences are also expected since the Wasatch Mountains are closer to GSL and thus should receive more dust from GSL. Notably, in all cases SDL was a more important dust source than GSL, even at the northernmost sampling sites, in part because SDL covers a larger surface area than the dust-producing areas of GSL. However, with ongoing declines in the GSL water level there could be relatively greater amounts of GSL dust in the future.

Seasonal differences in the inputs of GSL dust suggest that the relative importance of the GSL lakebed as a dust source may change depending on meteorological patterns or surface conditions on the lakebed. Higher $^{87}Sr/^{86}Sr$ ratios of urban dust during fall 2015 and fall 2018 may reflect seasonal wind patterns or drier conditions on the GSL lakebed during fall, leading to a greater input of GSL dust to the Wasatch Front. While the inputs of GSL dust to SLC, Ogden, and Logan changed across sampling periods, during most sampling periods GSL dust did not impact Provo. For snowpack, the Wasatch Mountains received more dust from GSL relative to the Uinta Mountains during all 3 years.

While the two-endmember mixing model is a first approximation at dust source apportionment for the Wasatch Front, a three-endmember mixing model including SDL, GSL, and other playas would more accurately predict dust contributions from playa sources. However, it is not possible to solve the equation for three endmembers because there is not a unique solution. An independent method for assessing contributions from each source is needed, which could then be tested with $^{87}Sr/^{86}Sr$ data. It is possible that atmospheric transport modeling could be an independent test of dust production from various sources.

To show how modeling and isotopic data could complement one another, we provide an example of applying $^{87}Sr/^{86}Sr$ ratios as a check on modeling studies. A modeling study for a dust storm on 13–14 April 2017 predicted that the dust deposited to snowpack near Alta, Utah, contained a mixture of 21% SDL dust, 7% GSL dust, and 72% dust from other playas (Skiles *et al* 2018). For this dust event, we measured an $^{87}Sr/^{86}Sr$ ratio of 0.71078 in dust from Alta snowpack (supplementary material, table S1, sample 13 754). Our two-endmember mixing calculations indicate that this dust layer contained 15% GSL dust, higher than the 7% contribution predicted by the modeling study. A three-endmember mixing model, using dust contributions from the modeling study (21% SDL dust, 7% GSL dust, and 72% dust from other playas) and average $^{87}Sr/^{86}Sr$ ratios values from SDL (0.71008), GSL (0.71476), and other playas (0.71178), results in a $^{87}Sr/^{86}Sr$ ratio of 0.71163. This value of 0.71163 calculated using dust proportions from the model is higher than the measured value of 0.71078 in the dust layer. We can more closely match the model results by either (1) decreasing the amount of GSL dust with a corresponding increase in SDL dust or (2) increasing the amount of SDL dust and decreasing the amount of dust from other playas. Since GSL dust likely does affect local snowpack to some extent, we assume that option 2 is more reasonable and use a nominal value of 7% GSL dust as predicted by the model. With option 2, we can match the observed $^{87}Sr/^{86}Sr$ ratio of the dust layer with a combination of 73% SDL dust, 7% GSL dust, and 20% dust from other playas. Thus, the model likely underpredicted the amount of SDL dust and overpredicted the amount of dust from other playa sources. This

may be because the dust transport model was unable to account for playas that were covered by temporary standing water, resulting in predicted emissions from areas where dust production was unlikely, as noted in Skiles *et al* (2018).

This example of comparing measured $^{87}Sr/^{86}Sr$ ratios to results from modeling studies, using an iterative process, shows that this may be a powerful tool for dust apportionment in northern Utah. More examples are needed to verify that this method could be used for different dust storms. By coupling $^{87}Sr/^{86}Sr$ data with modeling studies, we could better quantify GSL dust using an iterative approach. The isotopic data could also be used to validate and refine dust transport models. The feedback between geochemical observations and dust transport models would greatly improve dust apportionment studies and source tracking in northern Utah and other areas affected by regional playa dust sources.

5. Conclusion

Tracking dust from playas to urban areas and mountain snowpack is increasingly important with the desiccation of lakes worldwide. In our study, we show how the $^{87}Sr/^{86}Sr$ ratio in the carbonate mineral fraction of playa dust can be used to quantify dust contributions from playas to downwind areas. Unique $^{87}Sr/^{86}Sr$ ratios of western Utah playas, ranging from ~0.710 at SDL to ~0.715 at GSL, explained seasonal variability in $^{87}Sr/^{86}Sr$ ratios in the Wasatch Front urban area and snowpack of the Wasatch and Uinta Mountains. Our mixing model indicates that the dry lakebed of GSL contributed up to 34% of the dust flux to the northern Wasatch Front 22% of the dust flux to Wasatch Mountain snowpack during the study period. With the ongoing desiccation of GSL, these observations could have major impacts on understanding future dust emissions from the dry lakebed and impacts on downwind areas. The $^{87}Sr/^{86}Sr$ fingerprint of playa dust sources can be used to refine dust transport models to better quantify the amount of dust from GSL and other playas. To our knowledge, this is the first study to use $^{87}Sr/^{86}Sr$ ratios to trace dust from specific playas to downwind areas of deposition. The combination of $^{87}Sr/^{86}Sr$ fingerprints in carbonate minerals from playa dust and dust transport modeling may be the state-of-the-art for dust source apportionment in northern Utah and other areas impacted by regional playa dust sources.

Acknowledgments

This project was supported by the Utah Division of Forestry, Fire and State Lands and the US National Science Foundation grants EAR-1521468 and EAR-2012093. We thank Andrew Bentz and Natalie Barkdull for assisting with field work. We also thank Weber State University and Utah State University for providing access to their campuses for dust sampling. Jennifer DeGraffenried and Christopher Bradbury provided access to Dugway Proving Grounds.

Data availability statement

All data that support the findings of this study are included within the article (and any supplementary information files).

ORCID iD

Gregory T Carling https://orcid.org/0000-0001-5820-125X

References

Belnap J and Gillette D A 1997 Disturbance of biological soil crusts: impacts on potential wind erodibility of sandy desert soils in southeastern Utah *Land Degrad. Dev.* **8** 355–62

Biscaye P E, Grousset F E, Revel M, VAN DER Gaast S, Zielinski G A, Vaars A and Kukla G 1997 Asian provenance of glacial dust (stage 2) in the Greenland Ice Sheet Project 2 Ice Core, Summit, Greenland *J. Geophys. Res. Oceans* **102** 26765–81

Bullard J E, Harrison S P, Baddock M C, Drake N, Gill T E, Mctainsh G and Sun Y 2011 Preferential dust sources: A geomorphological classification designed for use in global dust-cycle models *J. Geophys. Res. Earth Surf.* **116** F04034

Capo R C and Chadwick O A 1999 Sources of strontium and calcium in desert soil and calcrete *Earth Planet. Sci. Lett.* **170** 61–72

Capo R C, Stewart B W and Chadwick O A 1998 Strontium isotopes as tracers of ecosystem processes: theory and methods *Geoderma* **82** 197–225

Carling G T, Fernandez D P and Johnson W P 2012 Dust-mediated loading of trace and major elements to Wasatch Mountain snowpack *Sci. Total Environ.* **432** 65–77

Chen J, Li G, Yang J, Rao W, Lu H, Balsam W, Sun Y and Ji J 2007 Nd and Sr isotopic characteristics of Chinese deserts: implications for the provenances of Asian dust *Geochim. Cosmochim. Acta* **71** 3904–14

Dastrup D B, Carling G T, Collins S A, Nelson S T, Fernandez D P, Tingey D G, Hahnenberger M and Aanderud Z T 2018 Aeolian dust chemistry and bacterial communities in snow are unique to airshed locations across northern Utah, USA *Atmos. Environ.* **193** 251–61

Engelbrecht J P and Derbyshire E 2010 Airborne Mineral Dust *Elements* **6** 241–6

Gill T E 1996 Eolian sediments generated by anthropogenic disturbance of playas: human impacts on the geomorphic system and geomorphic impacts on the human system *Geomorphology* **17** 207–28

Goodman M M, Carling G T, Fernandez D P, Rey K A, Hale C A, Bickmore B R, Nelson S T and Munroe J S 2019 Trace element chemistry of atmospheric deposition along the Wasatch Front (Utah, USA) reflects regional playa dust and local urban aerosols *Chem. Geol.* **530** 119317

Gross A, Palchan D, Krom M D and Angert A 2016 Elemental and isotopic composition of surface soils from key Saharan dust sources *Chem. Geol.* **442** 54–61

Hahnenberger M and Nicoll K 2012 Meteorological characteristics of dust storm events in the eastern Great Basin of Utah, U.S.A *Atmos. Environ.* **60** 601–12

Hahnenberger M and Nicoll K 2014 Geomorphic and land cover identification of dust sources in the eastern Great Basin of Utah, U.S.A *Geomorphology* **204** 657–72

Hahnenberger M and Perry K D 2015 Chemical comparison of dust and soil from the Sevier Dry Lake, UT, USA *Atmos. Environ.* **113** 90–97

Hart W S, Quade J, Madsen D B, Kaufman D S and Oviatt C G 2004 The 87Sr/86Sr ratios of lacustrine carbonates and lake-level history of the Bonneville paleolake system *Geol. Soc. Am. Bull.* **116** 1107–19

Jewell P W and Nicoll K 2011 Wind regimes and aeolian transport in the Great Basin, U.S.A *Geomorphology* **129** 1–13

Lawrence C R and Neff J C 2009 The contemporary physical and chemical flux of aeolian dust: A synthesis of direct measurements of dust deposition *Chem. Geol.* **267** 46–63

Lawrence C R, Painter T H, Landry C C and Neff J C 2010 Contemporary geochemical composition and flux of aeolian dust to the San Juan Mountains, Colorado, United States *J. Geophys. Res* **115** G03007

Mackey G and Fernandez D 2011 High throughput Sr isotope analysis using an automated column chemistry system AGU Fall Meeting () San Francisco, CA

Mahowald N M *et al* 2010 Observed 20th century desert dust variability: impact on climate and biogeochemistry *Atmos. Chem. Phys.* **10** 10875–93

Mallia D V, Kochanski A, Wu D, Pennell C, Oswald W and Lin J C 2017 Wind-blown dust modeling using a backward-Lagrangian particle dispersion model *J. Appl. Meteorol. Climatol.* **56** 2845–67

Munroe J S 2014 Properties of modern dust accumulating in the Uinta Mountains, Utah, USA, and implications for the regional dust system of the Rocky Mountains *Earth Surf. Process. Landf.* **39** 1979–88

Munroe J S, Norris E D, Carling G T, Beard B L, Satkoski A M and Liu L 2019 Isotope fingerprinting reveals western North American sources of modern dust in the Uinta Mountains, Utah, USA *Aeolian Res.* **38** 39–47

Naiman Z, Quade J and Patchett P J 2000 Isotopic evidence for eolian recycling of pedogenic carbonate and variations in carbonate dust sources throughout the southwest United States *Geochim. Cosmochim. Acta* **64** 3099–109

Neff J C, Ballantyne A P, Farmer G L, Mahowald N M, Conroy J L, Landry C C, Overpeck J T, Painter T H, Lawrence C R and Reynolds R L 2008 Increasing eolian dust deposition in the western United States linked to human activity *Nat. Geosci.* **1** 189–95

Nicoll K, Hahnenberger M and Goldstein H L 2020 'Dust in the wind' from source-to-sink: analysis of the 14–15 April 2015 storm in Utah *Aeolian Res.* **46** 100532

Oviatt C G 1988 Late Pleistocene and Holocene lake fluctuations in the Sevier Lake basin, Utah, USA *J. Paleolimnol.* **1** 9–21

Oviatt C G and Shroder J F 2016 Introduction *Developments in Earth Surface Processes* eds C G Oviatt and J F Shroder (Amsterdam: Elsevier)

Painter T H, Deems J S, Belnap J, Hamlet A F, Landry C C and Udall B 2010 Response of Colorado River runoff to dust radiative forcing in snow *Proc. Natl Acad. Sci. USA* **107** 17125–30

Palchan D, Stein M, Almogi-labin A, Erel Y and Goldstein S L 2013 Dust transport and synoptic conditions over the Sahara–Arabia deserts during the MIS6/5 and 2/1 transitions from grain-size, chemical and isotopic properties of Red Sea cores *Earth Planet. Sci. Lett.* **382** 125–39

Reheis M C 1997 Dust deposition downwind of Owens (dry) Lake, 1991–1994: preliminary findings *J. Geophys. Res. Atmos.* **102** 25999–6008

Reheis M C, Budahn J R and Lamothe P J 2002 Geochemical evidence for diversity of dust sources in the southwestern United States *Geochim. Cosmochim. Acta* **66** 1569–87

Reheis M C, Budahn J R, Lamothe P J and Reynolds R L 2009 Compositions of modern dust and surface sediments in the Desert Southwest, United States *J. Geophys. Res. Earth Surf.* **114** 20

Reheis M C and Kihl R 1995 Dust deposition in southern Nevada and California, 1984–1989: relations to climate, source area, and source lithology *J. Geophys. Res. Atmos.* **100** 8893–918

Reynolds R L *et al* 2014 Composition of dust deposited to snow cover in the Wasatch Range (Utah, USA): controls on radiative properties of snow cover and comparison to some dust-source sediments *Aeolian Res.* **15** 73–90

Skiles S M, Derek V M, Hallar A G, John C L, Andrew L, Ross P and Steven C 2018 Implications of a shrinking Great Salt Lake for dust on snow deposition in the Wasatch Mountains, UT, as informed by a source to sink case study from the 13–14 April 2017 dust event *Environ. Res. Lett.* **13** 124031

Steenburgh W, Massey J D and Painter T H 2012 Episodic dust events of Utah's Wasatch front and adjoining region *J. Appl. Meteorol. Climatol.* **51** 1654–69

Steiger R H and Jäger E 1977 Subcommission on geochronology: convention on the use of decay constants in geo- and cosmochronology *Earth Planet. Sci. Lett.* **36** 359–62

Wurtsbaugh W A, Miller C, Null S E, Derose R J, Wilcock P, Hahnenberger M, Howe F and Moore J 2017 Decline of the world's saline lakes *Nat. Geosci.* **10** 816

Zdanowicz C, Hall G, Vaive J, Amelin Y, Percival J, Girard I, Biscaye P and Bory A 2006 Asian dustfall in the St. Elias Mountains, Yukon, Canada *Geochim. Cosmochim. Acta* **70** 3493–507

Zhao W, Sun Y, Balsam W, Zeng L, Lu H, Otgonbayar K and Ji J 2015 Clay-sized Hf-Nd-Sr isotopic composition of Mongolian dust as a fingerprint for regional to hemispherical transport *Geophys. Res. Lett.* **42** 5661–9